ELSEVIER

Contents lists available at ScienceDirect

## Minerals Engineering

journal homepage: www.elsevier.com/locate/mineng





# Tannin: An eco-friendly depressant for the green flotation separation of hematite from quartz

A. Tohry <sup>a</sup>, R. Dehghan <sup>a,\*</sup>, Laurindo de Salles Leal Filho <sup>b</sup>, S. Chehreh Chelgani <sup>c</sup>

- <sup>a</sup> Mineral Processing, Department of Mining and Metallurgical Engineering, Yazd University, 89195-741 Yazd, Iran
- b Laboratory of Transport Phenomena and Chemistry of Interfaces, Department of Mining and Petroleum Engineering, Av. Prof. Mello Moraes 2237, University of São Paulo, São Paulo, Brazil
- <sup>c</sup> Minerals and Metallurgical Engineering, Department of Civil, Environmental and Natural Resources Engineering, Luleå University of Technology, SE-971 87 Luleå, Sweden

#### ARTICLEINFO

#### Keywords: Tannin Hematite Quartz Selective flotation Surface adsorption

#### ABSTRACT

Reverse cationic flotation is the most known beneficiation method for the separation of fine hematite particles from silicates. In this process, the depression of the hematite surface is an essential factor. Thus, the development of environmentally friendly depressants plays a critical role. Tannin (TA) as a natural and eco-friendly organic reagent has not yet been considered for such a purpose. Through the reverse cationic flotation, the depression effect of TA was investigated by single and mixture of minerals. Micro-flotation tests and wettability analysis based on contact angle measurements by the captive bubble method (CBM) were conducted. The surface adsorption mechanism of TA on the hematite and quartz was explored through turbidity, zeta-potential measurements, surface adsorption tests, and Fourier transform infrared (FT-IR) analyses. The micro-flotation results indicated that TA could selectively depress more than 90% of hematite, while its effect on quartz floatability was negligible (<8% depressing). Surface wettability analysis demonstrated that TA in the presence of 30 mg/L collector could significantly increase the work of adhesion of hematite from 135.5 to 143.1 erg/cm<sup>2</sup>, whereas it increased the work of adhesion of quartz from 117.1 to 120.7 erg/cm<sup>2</sup>. Surface adsorption analysis depicted that in the presence of 100 mg/L TA, the adsorption amount of TA on the hematite surface was 0.99 mg/g, while this amount for quartz was 0.17 mg/g (around 6 times lower than hematite). Turbidity measurements, applied to clarify the aggregation - dispersion behavior of pure minerals in the TA presence, showed that TA had a dispersion effect on the quartz particles, whereas TA caused hematite aggregation. Surface analyses proved that TA selective adsorption occurred on the hematite surface mainly by chemisorption. In contrast, poor physical adsorption was the main interaction between TA and the quartz surface.

## 1. Introduction

Reverse cationic flotation is known as the most efficient method to recover and separate fine iron oxides (hematite) from their associated minerals (silicates) (Manser, 1975; Araujo et al., 2005; Filippov et al., 2014; Gibson et al., 2017; Fan et al., 2020; Tohry et al., 2021a). This process is only efficient when iron oxides are selectively depressed (Kar et al., 2013; Tohry and Dehghani, 2016; Veloso et al., 2018). The main role of depressants in the flotation of iron oxides is to hinder the adsorption of collectors on the surface of iron-bearing minerals (deactivate their surfaces), while having minimal adsorption on the gangue surfaces. Macromolecular depressants are widely known as useful reagents to depress iron oxide minerals in reverse cationic flotation

(Pavlovic and Brandao, 2003; Turrer and Peres, 2011; Kar et al., 2013; Filippov et al., 2014; Fan et al., 2020; Tohry et al., 2021a). Among various organic and non-organic depressants such as starch (Pavlovic and Brandao, 2003; Araujo et al., 2005; Filippov et al., 2013), dextrin (Raju et al., 1998), sodium silicate and its derivatives (Tohry and Dehghani, 2016; Tohry et al., 2019, 2021b), guar gum (Zhao et al., 2017; Turrer and Peres, 2011), humic acid (Dos Santos and Oliveira, 2007; Tohry et al., 2021a), carboxymethylcellulose (CMC) (Shrimali and Miller, 2016; Poperechnikova et al., 2017), etc., starch typically has been introduced as the most successful depressant for iron oxide minerals (Pavlovic and Brandao, 2003; Kar et al., 2013; Filippov et al., 2014; Shrimali and Miller, 2016).

Starch is classified as a polysaccharide, a group which is frequently

E-mail address: rdehghans@yazd.ac.ir (R. Dehghan).

<sup>\*</sup> Corresponding author.

used for the reverse cationic flotation of iron ores (Pavlovic and Brandao, 2003; Araujo et al., 2005; Pearse, 2005; Ma et al., 2011; Turrer and Peres, 2011; Abdel-Khalek et al., 2012; Filippov et al., 2013; Kar et al., 2013; Filippov et al., 2014; Veloso et al., 2018; Shrimali and Miller, 2016; Bai et al., 2019; Fan et al., 2020). However, some studies have shown that starch and other polysaccharides adsorb on the quartz and other silicate mineral surfaces and render their surface hydrophilic (Filippov et al., 2013; Peçanha et al., 2019; Ming et al., 2020). This effect can be enhanced in the presence of Ca<sup>2+</sup> and Mg<sup>2+</sup> ions in the water process (Lelis et al., 2019). Moreover, it was reported that starch could depress some complex silicates through the reverse cationic flotation of iron oxides (Filippov et al., 2013; Veloso et al., 2018; Li et al., 2020). The gelatinization process (necessary for the preparation of starch solution) can also be considered another limitation (Araujo et al., 2005; Ma, 2012; Fan et al., 2020). In this process, a large quantity of NaOH or warm water is usually needed, leading to a high cost. Concerning these drawbacks, although starch is the most common industrial depressant for reverse cationic flotation of iron oxides, introducing potential alternatives is crucial (Zhang et al., 2019; Li et al., 2020).

Polyphenols (mainly humate derivatives), another family of macromolecular depressants, have been shown to be promising depressants for the iron oxides (Ramos-Tejada et al., 2003; Dos Santos and Oliveira, 2007; Zhang et al., 2012; Veloso et al., 2018; Tohry et al., 2021a). Humic acid as a binder in the pelletizing process has been used and found that it can strongly adsorb on the surface of iron oxides (hematite and magnetite), while its adsorption on the quartz surface has been reported to be negligible (Zhou et al., 2014; Zhou et al., 2015). In the acidic pH, preferential adsorption of sodium lignosulfonate, a type of polyphenol, on the hematite surface was reported, whereas its adsorption on the quartz surface was negligible (Engwayu, 2015). Tannins (TA) are a type of polyphenols, which have been considered for flotation separation of different ore/minerals such as phosphate ores (Al-Fariss et al., 1992), jamesonite (Chen et al., 2011), sulfides (Sarquís et al., 2014), minerals containing strontium (Rutledge and Anderson, 2015), calcite and pyrite (Rutledge, 2016), chalcopyrite and pyrite (Han et al., 2020). TAs have a complex mixture of natural and non-toxic polyphenols with no fixed molecular structure which have many uses in different industries, including the manufacture of leather (Pizzi, 2019), wood adhesives (Pizzi, 1983, 2019), pharmaceutical and medical applications (Noro et al., 1999, Pizzi, 2008), antioxidants (Audi et al., 1999), wastewater treatment (Yu et al., 2001).

They are mostly yielded via extraction from plants. Oxygencontaining functional groups in the structure of TAs facilitate their rapid and easy reactions with metallic ions (Rutledge and Anderson, 2015; Pizzi, 2019; Fraga-Corral et al., 2020). All these caused that TA absorbed attention for its application in mineral processing. There are some reports which reported TA potential for its industrial application in mineral processing and extractive metallurgy e.g., as a depressant of sulfide gangue minerals in the flotation of jamesonite (Chen et al., 2011), as adsorbent of ultrafine gold in bacterial oxidation method for treatment of primary sulfide refractory gold (Buah et al., 2015), as an adsorbent for precious metals from acidic leach liquor of circuit boards of spent mobile phones (Gurung et al., 2012). It has been proven that TA can be effectively used in the flotation of calcium-containing minerals and sulfides (Al-Fariss et al., 1992; Chen et al., 2011; Sarquís et al., 2014; Liu et al., 2016; Rutledge, 2016; Matveeva et al., 2017; Tangarfa et al., 2019; Han et al., 2020). However, as an eco-friendly reagent, the depression effect of TAs on iron oxides through the reverse cationic flotation separation from silicates and their adsorption mechanisms have not been addressed yet.

In this study, TA examined to depress hematite and separate it through reverse cationic flotation from quartz. For such a purpose, single micro-flotation tests were first done to expose the effects of TA concentrations and pH. Selective reverse cationic flotation of hematite from quartz was further examined using the mineral mixtures in the presence of ether amine as a cationic collector (in alkaline condition: pH

 $\sim$  9.2). Contact angle measurements in different collector concentrations were done to determine the wettability of minerals in the TA absence and presence. The adsorption mechanism of TA on both mineral surfaces was determined by turbidity, zeta-potential measurements, surface adsorption tests, and Fourier transforms infrared (FT-IR) analyses.

#### 2. Materials and methods

## 2.1. Mineral samples and chemicals

Pure hematite and quartz were sampled from "Ferriferous Quadrangle, Minas Gerais", and "Mineração Jundu from Descalvado-SP", Brazil, respectively. The high purity of the quartz sample (>98% of quartz) was confirmed by chemical analysis (Table I- Appendix A) and Xray diffraction (XRD) (Fig. I- Appendix A). The potassium dichromate titration method was used to analyze the Fe and FeO content of hematite. Based on the results, the high purity of hematite was also confirmed (total Fe  $\sim$  68.7%, FeO < 0.2% and SiO<sub>2</sub>  $\sim$  0.34%). Large pieces of the fresh minerals (both hematite and quartz) were selected by a visual survey to minimize cracks and impurities. They were kept for further cutting, polishing, and preparation of flat plates (diameter: 30.0 mm) for direct measurements of the contact angle by the captive bubble method (CBM). The rest of the samples were crushed by a hand-hammer and pulverized by a porcelain mortar. The size fraction of  $-75 + 25 \,\mu m$  was used for the micro-flotation and adsorption tests, while the  $-25\,\mu m$  size fraction was used for the zeta potential, turbidity, and FT-IR measurements.

As the hematite depressant, a commercial-grade TA was provided from TANAC S.A., Montenegro, Rio Grande do Sul, Brazil. TA used in this study is a commercial mixture of condensed tannins extracted from Acacia Mollissima tree bark (Southern Brazil). This type of TA bears many condensed polyphenols, preferably flavan-3–4-diol, which shows high molecular weight. TA, available in powder form, has a brown color including anionic character, free primary-care physician (PCP), minimum 93.5% active matter, and pH (aqueous sol. 20% w/v): 4.5–5.5. TA is soluble at room temperature, and it increases water viscosity and yields colloids (e.g., 40–45 wt%, 5 mPa s<sup>-1</sup> at 20 °C). The viscosity depends on the TA concentration, where a strong hydrogen bridge formed between the –OH groups and the water molecules is the main reason for this increase (Garcia et al., 2016).

A commercial-grade ether amine 50%, neutralized by acetic acid (Flotigam®EDA, Clariant, Sao Paulo, Brazil) was used as the cationic collector. Solutions of the analytical grade of HCl and NaOH were prepared at the concentration of 1% (w/v) and used for the pH adjustment to acidic (2–4) and alkaline (7–11) conditions in zeta potential measurements and the rest of the experiments. Analytical grade acetone ( $C_3H_6O$ ), and ethanol ( $C_2H_5OH$ ) were also used to clean the flat plate of quartz and hematite before applying the CBM (Tohry et al., 2020). Casa Americana, Brazil, supplied all these chemicals. Distilled water was used in all experiments except turbidity measurements. In the turbidity measurements, deionized water was considered. Detailed analysis of the used water components was revealed in Table II and Table III, Appendix A.

## 2.2. Micro-flotation tests

In order to perform micro-flotation tests with well-defined pH and TA concentration, two divided series of tests were carried out. At the initial step, 5 tests were performed in the pH range of 7–10 to find the optimum flotation pH (in the presence of TA) for maximizing the hematite recovery. It has been reported that in the pH range of 8–12, phenolate anions are in equilibrium in an aqueous solution (Smith and March, 2007; Garcia et al., 2016). These anions have a great tendency to metallic cations (Matveeva et al., 2016, 2017; Tangarfa et al., 2019; Fraga-Corral et al., 2020). In the second stage, the optimum TA

**Table 1**Comparison between hematite: quartz ratios (used as the mixture minerals for the micro-flotation tests), and typical iron ores find worldwide.

Hematite : Quartz mixture		Ore type	Reference	
Ratio	Total Fe (%)	Origin	Charactrization	
80 : 20	55.1	Samarco mining complex, Minas Gerais, Brazil	$53\%$ total Fe, $20$ – $23\%$ $SiO_2$ (quartz)	Houot, 1983
		Sawyer Lake deposit, Schefferville, Canada	High-grade hematite containing 80% hematite with intergranular quartz	Conliffe, 2014
60:	41.3	Banded Iron	54.4% hematite,	Ramakgala &
40		Formation (BIF) deposit, Central part of Botswana, South	44.0% quartz, 1.1% magnetite and 0.5% goethite minerals	Danha, 2019
		Aferica		
		Sanje iron ore,	48.9% hematite	Siame et al.,
		Nampundwe area of	(34.2% total Fe)	2019
		Zambia, East Africa	containing 38% SiO <sub>2</sub>	
40:	27.6	BIF ores, Odisha iron	Hematite (35-40%),	Krishna et al.,
60		ore mine, India	cherty quartz	2013
			(60–65%), 26.5%	
			total Fe, 61.2% SiO <sub>2</sub>	
		Yeravninskiy iron	40% hematite, 60%	Konovalov,
		ore deposit, Russia	quartz	1970
		East Anshan	38% hematite (30.5%	Song et al.,
		hematite ore, China	total Fe), 55.5%	2002
		T 4	quartz	Seifelnassr
		Iron ore deposit at Wadi Halfa area.	45.3% hematite, SiO <sub>2</sub> content: 47.5%	
		Sudan, Northeast Africa	content: 47.5%	et al., 2013

concentration was determined by applying the defined pH at the first step. At this stage, tests were conducted in the presence of 10, 60, 70, 80, 90, 100, and 150 mg/L TA. Finally, by knowing the desirable pH and TA concentration, single micro-flotation tests were performed in the presence of different concentrations of Flotigam®EDA. Micro-flotation of the mineral mixture was also carried out by considering the optimum conditions obtained in the single mineral micro-flotation tests.

Each micro-flotation test was repeated three times in a Hallimond tube with 60 mL volume, and the average results are given in the results. Water was used as a background solution in all experiments because of its widespread use in industrial flotation circuits to separate minerals. A mechanical stirrer was used at a fixed speed of 1380 rpm. It has been reported (Rodrigues and Leal Filho, 2010) that maximum recovery of apatite and glass spheres was achieved in the Froude number range (Fr) of 0.1-0.6, where stirrer diameter/Hallimond tube diameter was equal to 0.7. Regarding the choice of stirrer rotational speed in mentioned research, 1380 r/min was considered in this study. Nitrogen gas, at the rate of 50 mL/min, was used in order to generate bubbles (Martinz, 2009; Davidson, 2009; Mphela, 2010; Liu et al., 2017; Souza and Lima, 2019; Lu et al., 2020). During each micro-flotation test, 1.0 g sample and around 55 mL pre-adjusted water with the desired pH were mixed in the micro-flotation cell. The slurry was conditioned by stirring for 1 min before the TA was added and conditioned for 3 min by stirring (except for the test without depressant), finally the collector at the desired concentration was added to the slurry and conditioned for 1 min. After conditioning, flotation was performed for 1 min, as proposed by Rodrigues and Leal Filho (2010), Lelis et al. (2016), Silva et al. (2019). The flotation products were collected by hand scraping rates of once every 2-3-second, filtered, dried at 40 °C and weighted separately, and the weight recovery was calculated. For the micro-flotation of the mixed minerals, the procedure was the same as the single mineral microflotation tests.

The examined mineral mixture tests were done in 3 different "hematite: quartz" weight ratios of 40:60, 60:40, and 80:20. Weight ratios

are considered for simulating the low grade and high-grade iron ores containing silica, in which weight ratios of 40:60, 60:40, and 80:20 are indicating 27.6, 41.3, and 55.1% total Fe, respectively. In general, similar ratios for iron ore deposits containing silica could be observed worldwide (Table. 1). After yielding the flotation products, they were analyzed by potassium dichromate titration method to measure the total Fe content.

#### 2.3. Wettability

The surface wettability of hematite and quartz was characterized by the contact angle measurements in the presence and absence of reagents. Goniometer DSA25 (supplied by Kruss, Germany) was adopted to carry out the contact angle measurements by the CBM. For the contact angle measurement, an air bubble was gently placed by a glass syringe endowed with a needle of diameter 0.487 mm on the mineral plate surface that pre-conditioned with collector and depressant. At least 4 created contact angle values were considered for each measurement. All measurements were done at 22  $\pm$  1  $^{\circ}$ C. For providing an accurate contact angle measurement, the points of intersection (the three-phase contact points of the system between the fitted bubble shape and the baseline) are measured automatically by the Kruss program, Young-Laplace, ellipse, and circle fitting models that can fit the bubble boundary line and contour line are typical models for such an assessment. It was well understood that for measuring higher contact angle values, mostly above 40°, ellipse fitting is more accurate and for small angles, Young-Laplace is the most reliable model. In the absence of TA, hematite, and quartz contact angles were measured with different concentrations of Flotigam®EDA (0, 2.5, 7.5, 15, and 30 mg/L). All these measurements were also repeated in the optimum pH and TA dosage, defined in microflotation tests, as well.

Means of the measured contact angles and their standard deviations for each experimental condition were applied in Eqs. (1) and (2) for calculating the work of adhesion and spreading coefficient values where  $W_a = \text{work}$  of adhesion (erg/cm²), S = spreading coefficient (erg/cm²),  $\theta = \text{contact}$  angle (degrees),  $\gamma_{LV} = \text{surface}$  tension of water (mN/m). The surface tension of distilled water was measured by a K100 Force tensioneter (Kruss, Germany). The standard deviation of work of adhesion and spreading coefficient (deduced by the laws of error propagation, according to Martinz, 2009) were calculated by Eqs. (3) and (4), respectively. where  $\sigma_{\gamma} = \text{water}$  surface tension standard deviation and  $\sigma_{\theta} = \text{contact}$  angle standard deviation.

$$W_a = \gamma_{LV}(\cos\theta + 1) \tag{1}$$

$$S = \gamma_{LV}(\cos\theta - 1) \tag{2}$$

$$\sigma_{W_a} = \sqrt{\sigma_{\gamma}^2 (1 + \cos[\theta])^2 + \gamma^2 \sigma_{\theta}^2 \sin[\theta]^2}$$
 (3)

$$\sigma_{S} = \sqrt{\sigma_{r}^{2}(\cos[\theta] - 1)^{2} + \gamma^{2}\sigma_{\theta}^{2}\sin[\theta]^{2}}$$
(4)

## 2.4. Adsorption experiments

Adsorption experiments were conducted using the solution depletion method. 1.0 g of each pure mineral was added to a 40 mL solution (in a 250 mL Erlenmeyer flask) with a known concentration of TA, and the pH value was set at the desired value. The flasks were placed in a digital horizontal shaker and agitated at 220 rpm for 2 h (at 22  $\pm$  1  $^{\circ}$ C). The flasks were kept standing (without shaking) for 1 h to settle the suspended solids naturally. The supernatant was withdrawn with a 25 mL pipette, centrifuged at 6,000 rpm for 30 min in a laboratory centrifuge, and then the remaining TA concentration was measured by Helios Alpha UV–VIS Spectrophotometer from Thermo gamma metric (England) at a wavelength of 279 nm to determine the residual TA in solution. The adsorption of TA on the mineral surfaces was calculated from the

difference between the original and residual concentrations (Eq. (5)).

$$q_e = \frac{(C_1 - C_2) V}{m} \tag{5}$$

Where  $q_e$  is the equilibrium adsorption capacity of adsorbent (mg/g), V is the volume of the solution (L),  $C_1$  and  $C_2$  are the initial and final concentrations of TA (mg/L), and m is the weight of the minerals added into the solution (g).

Freundlich (Eq. (6)) and Langmuir (Eq. (7)) adsorption isotherms were used for realizing the adsorption mechanisms between minerals and TA. By plotting  $\log q_e$  against  $\log C_e$  in the Freundlich model and plotting  $1/q_e$  against  $1/C_e$  in Langmuir model, factors of n and  $K_F$  (mg/g(L/mg)<sup>1/n</sup>) for Freundlich model and  $q_m$  (mg/g) and  $K_L$  (L/mg) factors for Langmuir adsorption isotherm can be achieved, respectively.

$$\log q_{\rm e} = \log K_{\rm F} + \frac{1}{n} \log C_{\rm e} \tag{6}$$

$$\frac{1}{q_e} = \frac{1}{q_m} + \frac{1}{K_L q_m} \frac{1}{Ce} \tag{7}$$

## 2.5. Zeta potential measurements

Zeta potential measurements were performed using a Malvern zeta sizer (nano – ZS90).  $50\pm1$  mg mineral sample was added to a 100 mL solution with the adjusted pH, and reagent concentrations (different for each experiment). The suspension was conditioned by magnetic stirring for 3 min. During the conditioning, the pH value was checked and kept constant. During the solution conditioning, a pH-meter electrode was located inside the solution, and the pH value was monitored, continually. The pH was kept constant by dipping an impregnated needle with the pH modifier. The suspension was left to stand for 5 min to allow the settling of the particles. The supernatant was removed (around 3 mL) and used for the zeta potential measurement. All of the experiments were conducted at  $22\pm1$  °C, and the results were the mean of three repeated measurements. Zeta potential measurements were performed at TA concentrations of 10, 30, 60, 100 and 150 mg/L at pH  $\sim$  9.2 and pHs of 2, 4, 7, 9 and 11 in the presence of 100 mg/L TA or its absence.

## 2.6. Turbidity measurements

Turbidity could give information on the state of dispersion or agglomeration of powders in a liquid. Knowing these two phenomena can help determine the mechanism of interaction between mineral particles and reagents in an aqueous solution. Turbidity measurements were performed by a Thermo Scientific turbidity meter (Model: AQUAfast II Orion AQ2010). Exactly 1.0 g of each pure mineral was added to a 100 mL pre-conditioned solution (in different TA concentrations at pH  $\sim$  9.2), and then stirred for 3 min. After that, the suspensions were kept standing for 5 min to allow particle settling, and then 10 mL supernatant (from a constant height for all solutions) was picked as experimental samples. All measurements were done at 22  $\pm$  1  $^{\circ}$ C.

## 2.7. FT-IR spectroscopy

FT-IR was used to detect the molecular environment and the composition of the TA functional groups on the surface of pure minerals before and after conditioning. The FT-IR analyses were performed with a Bruker Equinox-55 FT-IR analyzer (Germany) in the scanning range between 400 and 4000  ${\rm cm}^{-1}$ . For conditioning samples, 1.0 g of each pure sample was added into an aqueous solution of TA (100 mg/L), and conditioned for 2 h (pH  $\sim$  9.2). Particles were filtered and dried at room temperature for 24 h. The mineral sample was mixed with potassium bromide, by 1% weight ratio, at room temperature, and the spectra were recorded at a resolution of 4  ${\rm cm}^{-1}$ . The spectra of pure minerals, before

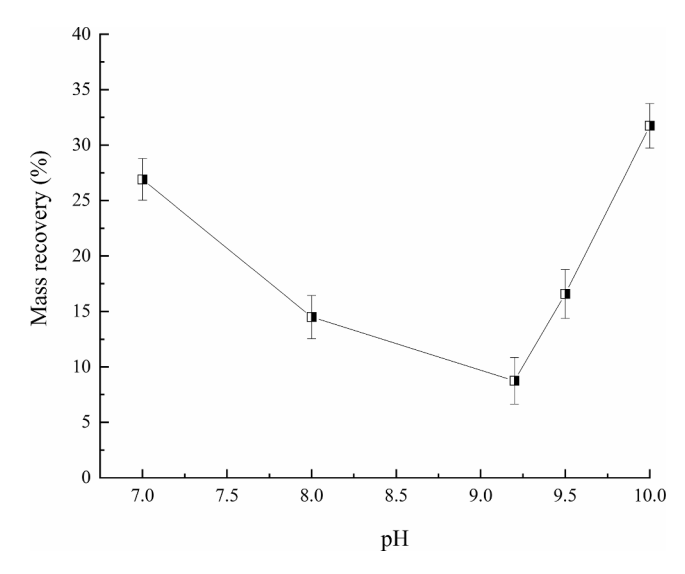


Fig. 1. Effect of TA on the floatability of pure hematite (in the presence of 30 mg/L Flotigam®EDA and 100 mg/L TA) at different pH values.

treatment by TA, were measured for comparison purposes.

#### 3. Results and discussion

## 3.1. Micro-flotation

In order to determine the optimum pH value for maximizing the depressing effect of TA on the hematite, micro-flotation tests were performed in different pHs with 100 mg/L TA and 30 mg/L Flotigam®EDA (Fig. 1). Since in the reverse cationic flotation of iron ores, the main goal is to achieve the maximum recovery of iron oxides in the immersed phase along with considering the lowest destructive effects on floatability of gangue minerals, a relatively high value of the depressants (100 mg/L) should be considered for the process (Vidyadhar et al., 2002; Filippov et al., 2013; Severov et al., 2016; Shrimali et al., 2018; Meng et al., 2019; Tohry et al., 2021b). Moreover, it has been reported that in concentrations more than 1.0 \* 10<sup>-4</sup> M of cationic collectors, maximum floatability of most silicate minerals can be achieved (Filippov et al., 2013; Filippov et al., 2014; Severov et al., 2016; Tohry et al., 2021a). Thus, 30 mg/L (1.4 \*  $10^{-4}$  mol/L with regarding molecular weight of 215.37 g mol<sup>-1</sup>) for Flotigam®EDA (Nunes et al., 2011), was considered. On the other hand, considering such concentration, the depressant selectivity on both gangue and valuable minerals will be clearly defined.

The experimental results indicated that in the pH region from 8 to 9.2, hematite was well depressed with TA. However, at pH 9.2, hematite recovery in the froth phase met its lowest level (around 9%). On the other hand, since the optimum pH range for efficient flotation separation of silicate gangues with cationic collectors is located in the range of 9–10.5 (Smith, 1963; Laskowski, 1989; Manser, 1975; Vieira and Peres, 2007; Filippov et al., 2010), the pH value of 9.2 was selected to conduct all the other experiments. The pH value above 9.2 caused further hematite particles to find their way into the froth phase (around 34% floated at pH 10). As mentioned, TA bears phenolic groups (–OH), and the dissociation of these functional groups occurs in the pH range 9–9.5 (Garcia et al., 2016). Eq. 8 shows the reaction of phenol dissolution to phenolate at the alkaline pH:

$$Phenol + H_2O = Phenolate + H_3O^+$$
 (8)

It has been documented that polyphenols during interaction with water in the neutral and alkaline pHs dissociated to the negatively charged components such as -HO<sup>-</sup> and -COO<sup>-</sup>. In the case of TA, hydroxy groups at alkaline pH (depend on dissociation constant of reagents containing phenolic groups) converted to phenoxide ion/phenolate

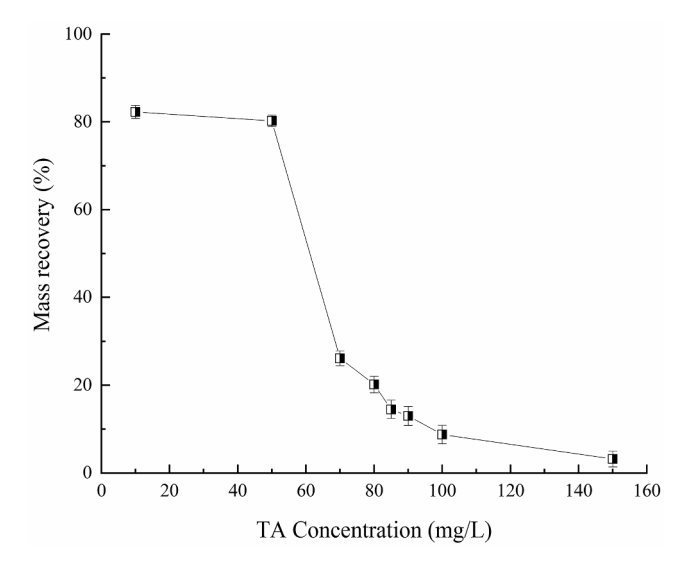


Fig. 2. Effect of TA concentration on the hematite recovery at pH 9.2 and 30 mg/L Flotigam®EDA.

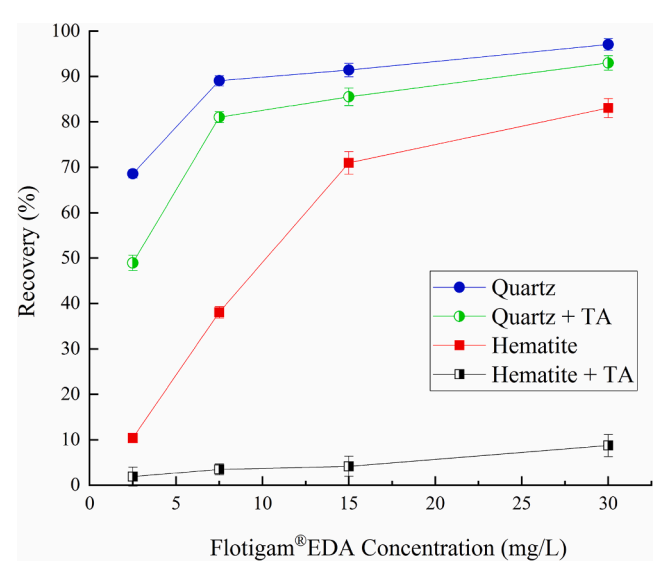
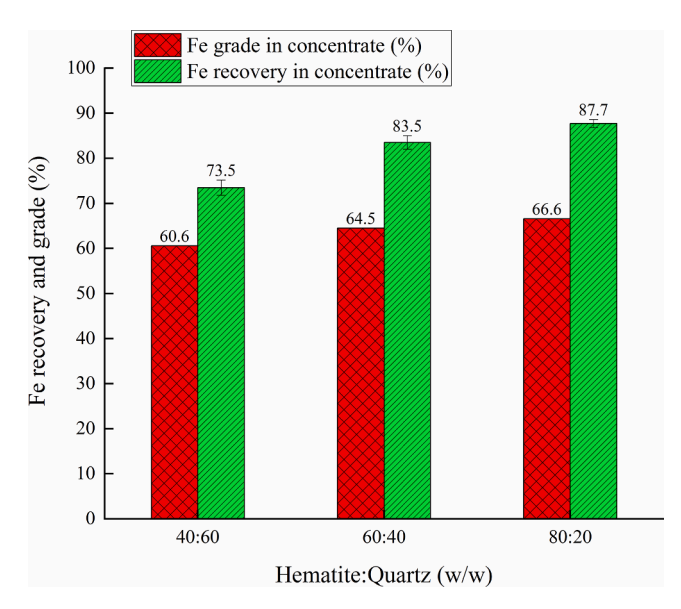


Fig. 3. Floatability of hematite and quartz as a function of Flotigam®EDA concentration at pH  $\sim$  9.2 (in the presence and absence of 100 mg/L TA).

(negative agents). Consequently, a greater tendency was formed to interact with other ions, i.e., Fe ion (Hem, 1960; Norgren and Lindström, 2000; Matveeva et al., 2016; Matveeva et al., 2017; Tangarfa et al., 2019; Fraga-Corral et al., 2020). Indeed, in our case, at pH  $\sim$  9.2, the concentration of non-ionic species (phenol) equals anionic species (phenolate); thus, the repulsion between phenol and phenolate groups on the hematite surface could be minimized. These phenomena maximized the adsorption of tannin on the hematite surface. At pH > 9.5, TA molecules became increasingly negative, and the zeta potential of hematite rendered increasingly negative, as well. Electrostatic repulsion between hematite and TA was expected to occur. On the other hand, the increasing scarcity of FeOH groups on the hematite surface as well as phenol groups in bulk aqueous solution jeopardized interaction between TA and hematite. Hem (1960) also reported that at pH 10, parts of tannic acids are undissociated and unavailable for complexing. Due to the lack of TA adsorption on the hematite surface, hematite interacts with collector molecules and floats. Since at pH around 9.2, a strong interaction between the hematite surface and TA occurred, and TA significantly depressed hematite (a desirable result for the reverse flotation), this pH



**Fig. 4.** Iron recovery and Fe grade of achieved iron concentrate from hematite and quartz mixtures flotation (in the presence of 30 mg/L Flotigam®EDA, 100 mg/L TA, and pH value of 9.2).

value was selected to conduct all the other experiments.

Micro-flotation test results also showed that by increasing the TA concentration at a constant pH of 9.2, the hematite recovery in the immersed phase was increased (Fig. 2). There is a lack of TA molecules in the low TA concentrations (<50 mg/L) to adsorb on the hematite surface (Fig. 2), and to depress it. This led to the recovery of more than 80% of hematite particles by the cationic collector. However, as the TA concentration in flotation solution increased from 50 to 70 mg/L, the adsorption of TA molecules on the hematite surface was increased significantly, and eventually, the hematite recovery sharply decreased. Hematite recovery in the immersed phase reached around 91% and 96% in the presence of 100 mg/L and 150 mg/L TA concentration, respectively. These outcomes revealed that the TA was a powerful depressant in the reverse cationic flotation of hematite. Such strong depression of the hematite has also been reported by other phenolic compounds (Dos Santos and Oliveira, 2007; Veloso et al., 2018; Tohry et al., 2021a).

The flotation recoveries of the hematite and quartz were explored as a function of Flotigam®EDA concentration in the absence and presence of 100 mg/L TA (Fig. 3). It was shown that the quartz recovery in the whole range of Flotigam®EDA concentration was higher than the hematite. This result is consistent with previous studies where quartz higher floatability than iron oxides through the reverse cationic flotation was reported (Araujo et al., 2005; Filippov et al., 2013; Filippov et al., 2014). These outcomes illustrated that TA could negligibly depress quartz, whereas increasing the Flotigam®EDA concentrations showed a negligible effect on the hematite recovery. A slight depression effect of TA on the quartz surface could be related to the physical interaction between the silanol groups of quartz surface and TA molecules. Such an interaction between silanol groups of silicates and reagents containing phenolic hydroxyl groups has been reported by Zhou et al. (2014, 2015) and Tohry et al. (2021a).

Although using 15 mg/L of the collector could also lead to hematite depression, but in order to assess the maximum TA depression power, its depression effect was examined in the presence of 30 mg/L collector, where the maximum floatability of quartz and hematite were obtained in the absence of TA. In the presence of 30 mg/L Flotigam®EDA and 100 mg/L TA, the floatability of quartz was around 90%, and recovery of hematite in the froth phase was lower than 10%. These results established the selective depression effect of TA on the hematite through the reverse cationic flotation system.

Micro-flotation tests of the mixed pure minerals (different weight

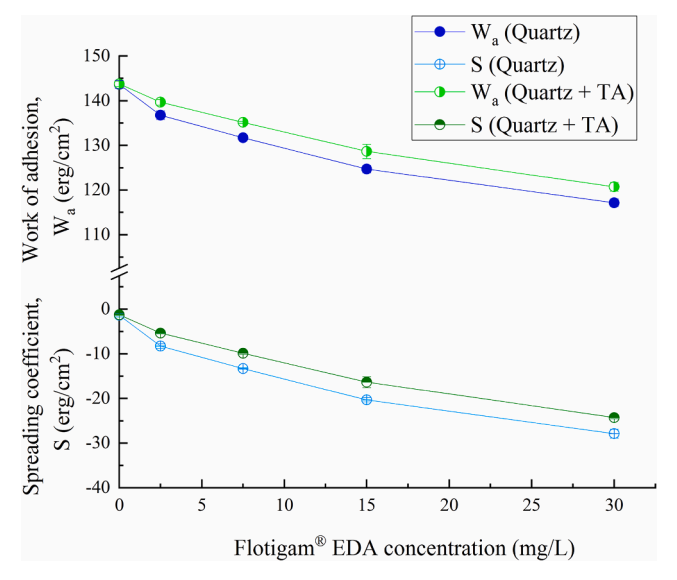


**Fig. 5.** Wettability parameters of quartz treated with and quartz treated with TA as a function of Flotigam®EDA concentration (in the presence of 100 mg/L TA and pH value of 9.2).

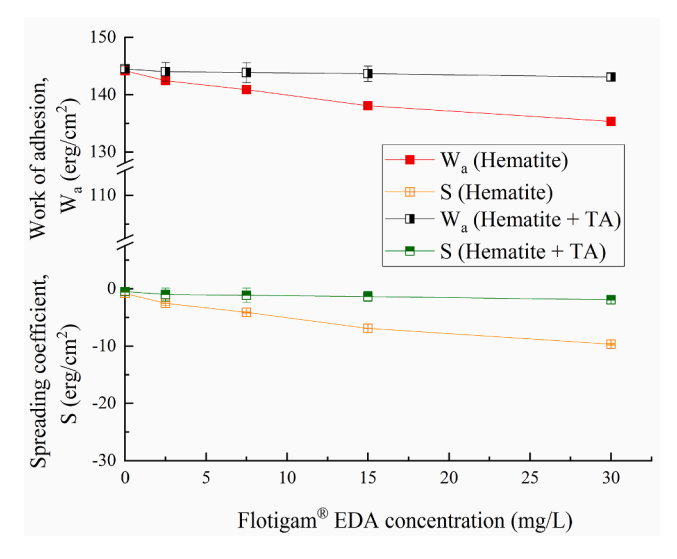


**Fig. 6.** Wettability parameters of hematite and hematite treated with TA as a function of Flotigam®EDA concentration (in the presence of 100 mg/L TA and pH value of 9.2).

ratios) demonstrated promising results for the efficient separation of hematite from quartz (Fig. 4). An incremental trend in the Fe grade and Fe recovery was observed by increasing its mass ratio (Fig. 4). In other words, by decreasing the mass ratio of quartz, in the mixtures, the metallurgical responses of reverse cationic flotation markedly improved. For instance, in the mass ratio of 80:20 (hematite: quartz), 1 stage flotation could achieve a concentrate with 66.6% Fe grade and 87.7% Fe recovery. It indicated that the addition of TA could selectively separate these two minerals by flotation.

## 3.2. Wettability results

The work of adhesion for quartz and hematite was calculated based on the contact angle as a function of Flotigam®EDA concentration (both in the presence and absence of TA). The outcomes (Figs. 5 and 6) illustrated that the work of adhesion for both quartz and hematite was decreased by increasing the collector concentration. This means

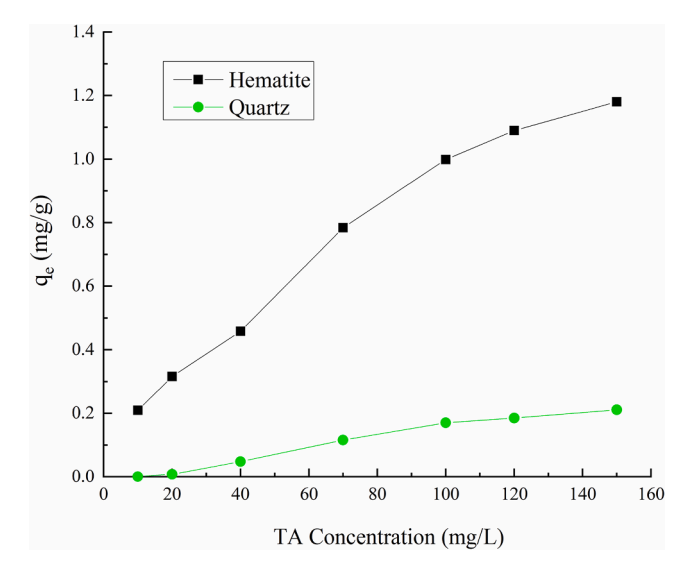


Fig. 7. Adsorption amount of TA on the hematite and quartz as a function of TA concentration (pH  $\sim$  9.2).

Flotigam®EDA decreased the hematite and quartz surface energy. These results agreed with Zhang et al. (2010) that showed the Wa values for an aqueous solution of cationic collectors decreased with an increase in their concentrations. The minimum Wa value was reported at the initial stage of the cationic surfactant bilayer formations at the quartz-water interface, where the cationic collector concentrations were relatively close to critical micelle concentration (CMC). These outputs are consistent with the micro-flotation results, where by increasing the collector concentration, the floatability of both quartz and hematite was increased (Fig. 3). The high hydrophobicity of both hematite and quartz in the presence of Flotigam®EDA was also reported in some investigations (Lelis et al., 2019, 2020), where quartz indicated a higher hydrophobicity than the hematite. Wettability results (Figs. 5 and 6), agreed well with the most recent studies (Lelis et al., 2019, 2020), which demonstrated the quartz surface energy all through the increasing the collector concentrations were significantly lower than the hematite. These facts depicted the higher interest of the treated quartz particles toward the air phase (more hydrophobic).

The spreading coefficient results (spreading of one liquid over solid phase) also indicated a similar pattern for these two minerals. Through flotation separation, a high negative spreading coefficient value is desirable (Leja, 1982). Results declared that at the same condition, the wetting of the hematite surface by water, in the presence of Flotigam®EDA is higher than the quartz surface. It meant that the quartz hydrophobicity was higher than the treated hematite, which confirmed the micro-flotation test outcomes. These phenomena could be due to the higher electrostatic attraction of ether aminium ions on the quartz surface than hematite. The contribution of the hydrogen bonds between the silanol groups on the quartz surface with the ether aminium ion could also be considered (Smith and Scott 1990; Churaev et al. 2000; Vidyadhar et al. 2002; Lelis et al., 2019).

These outcomes (Fig. 6) also revealed that the hematite treated with TA, had a greater work of adhesion than the hematite samples without TA, which should be translated to a greater affinity of the TA treated hematite to water. It showed that TA had a significant depressing effect on the surface of hematite, compared to the quartz, even in the presence of Flotigam®EDA. The spreading coefficient of the treated hematite with TA, in the collector presence, also confirmed its surface was getting completely wet. On the contrary, quartz had a different behavior (Fig. 5), where both its work of adhesion and spreading coefficient amounts in TA presence were less than the hematite. It was indicated that the addition of TA had a minor effect on the quartz wettability in the presence of Flotigam®EDA. It was consistent with the micro-flotation

**Table 2**Freundlich and Langmuir constants of TA adsorption on hematite and quartz surfaces.

Minerals	Freundlich parameters			Langmuir parameters			
	n	$K_{\mathrm{F}}$	$\mathbb{R}^2$	$q_m$	$K_{L}$	R <sup>2</sup>	
Hematite	1.79	$8.1 \times 10^{-2}$	0.99	1.03	5.0 × 10 <sup>-2</sup>	0.93	
Quartz	0.49	$1.0 \times 10^{-5}$	0.95	$5.0 \times 10^{-3}$	$1.5 \times 10^{-2}$	0.87	

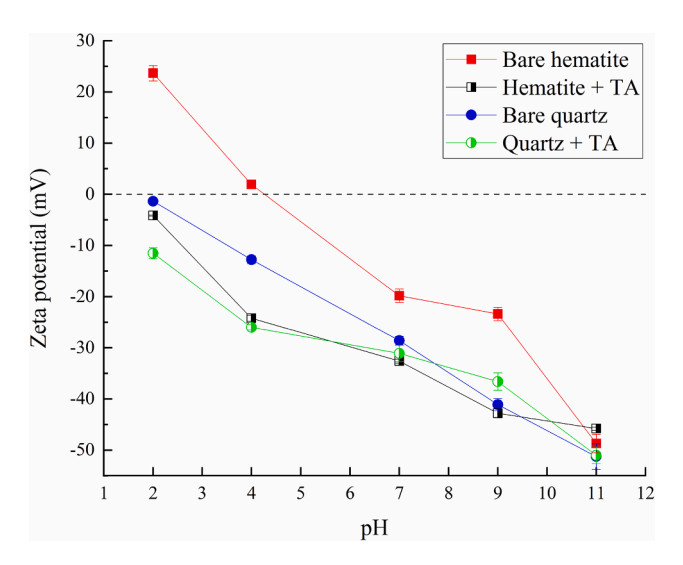


Fig. 8. Zeta potentials of hematite and quartz at different pH values in the presence of  $100\ mg/L$  TA.

results, where quartz still had excellent floatability even in the presence of TA (Fig. 3).

## 3.3. Surface adsorption results

The adsorption of TA on the quartz and hematite surface showed that the amount of the adsorbed TA on these mineral surface was enhanced when its equilibrium concentration was increased (Fig. 7). However, in the whole TA concentration range, the adsorption density of TA on the hematite surface was much higher than the quartz surface. When TA concentration reached 100 mg/L, the adsorption amount of TA on the hematite surface was 0.99 mg/g, while this amount for quartz (at the same concentration) was 0.17 mg/g (around 6 times lower than hematite), illustrating that TA had a strong adsorption interaction with the hematite surface compared to quartz. Tohry et al. (2021a) reported that the adsorption of polyphenol (Humic acid) on the iron oxide surface (hematite) is based on the formation of a chemical complex on its surface. In general, adsorption test results also proved that TA adsorbed more strongly on the surface of hematite than quartz, which is consistent with the other reported results.

Freundlich and Langmuir isotherm equations fitted the adsorption equilibrium data. The results (Table 2) depicted that the Freundlich isotherm model was more suitable to declare TA adsorption on the mineral surfaces due to its larger correlation coefficients. The value of n for hematite and quartz was obtained at 1.79 and 0.49, respectively. This implied that the interaction between hematite and TA is much stronger than quartz.

## 3.4. Zeta potential measurements

Based on the zeta potential measurements, the IEP (isoelectric point) of bare quartz and hematite occurred at pH  $\leq$  2 and around 4.2, respectively (Fig. 8). These results are in good agreement with the reported IEPs in other investigations (Leja, 1982; Carlson and Kawatra,

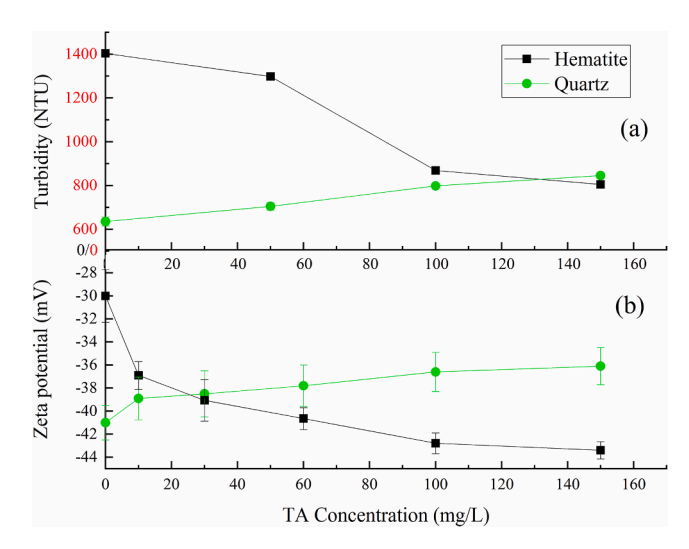


Fig. 9. Turbidity and zeta potential of hematite and quartz suspensions as a function of TA concentration at pH  $\sim$  9.2.

2013; Peçanha et al., 2019; Fan et al., 2020). Zeta potential values of hematite and quartz, over the investigated pH range and in the presence of 100 mg/L TA, were negative and became almost more negative by increasing the pH values. The same effects were documented for other depressants containing carboxylate and phenolic groups on the iron oxide and quartz surfaces (Zhang et al., 2012; Zhou et al., 2014, 2015). It was stated that carboxyl, phenolic hydroxyl, and hydroxyl groups in the polyphenol structure after ionization in a solution could lead to a negative charge on particle surfaces. These reagent ionizations increased in the alkaline condition and caused an intense zeta potential reduction (Zhang et al., 2012; Fraga-Corral et al., 2020; Han et al., 2020).

These results (Fig. 8) also demonstrated that TA adsorbed more strongly on the hematite surface than the quartz surface, due to the negative shifting of zeta potential of the treated hematite with TA, rather than the bare hematite, compared to the TA treated quartz. At pH 9.2, zeta potential of hematite changed from -23.37 mV to -42.80 mV ( $\Delta\zeta$  $\sim -19.43$  mV) and quartz shifted from -41.10 mV to -36.60 mV ( $\Delta \zeta \sim$ +4.50 mV). These variations indicated that the TA adsorption occurred on the hematite surface via a strong non-electrostatic/chemical interaction, while a weak physical interaction was dominant for quartz. However, the bare quartz surface showed a higher negative zeta potential than bare hematite, leading to a considerable electrostatic repulsion between quartz and the TA anionic species and reduce their adsorption. Zhou et al. (2014) showed a considerable electrostatic repulsion between anionic functional groups of humic acid, such as -COO<sup>-</sup>, and silanol groups of quartz. They concluded this phenomenon caused the insignificant adsorption of humic acid on the quartz surface (Zhou et al., 2014). It has also been reported that polyphenols exhibit a specific affinity for metal ions. They can easily interact with metal ions and act as a depressant for metallic minerals (Mahiuddin et al., 1992; Malan, 2015; Rutledge, 2016; Fraga-Corral et al., 2020). Since hematite is a metallic mineral containing a high density of Fe cations, it can accommodate TA higher adsorption on its surface compared to quartz.

## 3.5. Turbidity measurements

In order to acquire a better understanding of the mechanism of interaction of TA on the quartz and hematite, turbidity measurements were carried out in the presence of different TA concentrations at pH  $\sim$  9.2 (Fig. 9-a). The TA-treated quartz supernatant turbidity slightly increased by increasing the TA concentration, which meant the dispersity of quartz in the pulp was increased by adding this depressant. This result depicted that the treated quartz particles were stabilized via repulsive electrostatic forces between the charged particles. This point

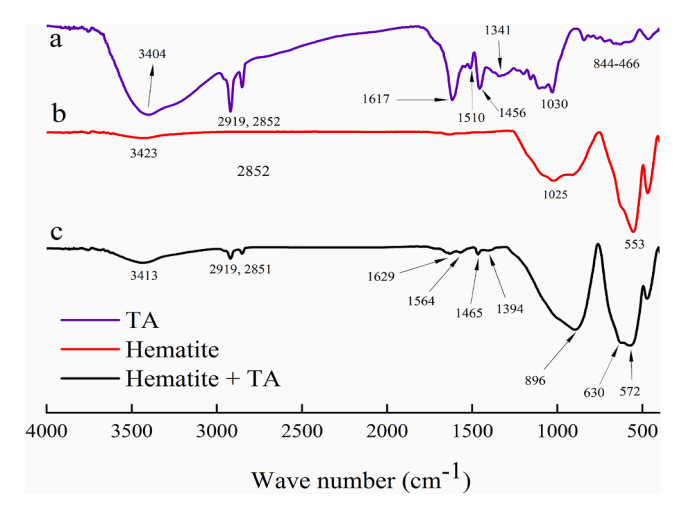


Fig. 10. FT-IR spectra of (a) TA, (b) hematite, and (c) hematite treated with  $100\ \text{mg/L}$  TA.

was also observed in another investigation (Engwayu, 2015), where it was indicated that lignosulfonate dispersed the silicate particles at both high and low pH values. By increasing the TA concentration, the zeta potential of quartz decreased slightly (Fig. 9-b). These results showed negligible TA adsorption on the quartz surface, which was in good agreement with the obtained results from adsorption and wettability experiments.

Unlike the quartz, hematite showed different behavior in the turbidity measurements, where by increasing the TA concentration, a decreasing trend in the hematite turbidity was seen (Fig. 9-a). This trend depicted that hematite particles aggregated with the addition of TA. This aggregation is expected to result in the hematite particles' flocculation, leading to improved surface wettability and hindering their flotation (Figs. 3, 5, and 6). This phenomenon, the depression of iron oxides by polysaccharides, has been widely reported (Schulz and Cooke, 1953; Pinto et al., 1992; Engwayu, 2015). The same was reported for the lignosulfonate interaction with hematite at pH 5.5 (Engwayu, 2015). It has been noted that the aggregation of a mineral in flotation is often beneficial to its depression (Engwayu, 2015, Shrimali et al., 2018; Gu et al., 2019). These results (Fig. 9-b) showed that by increasing the TA concentration, hematite zeta potential significantly increased, which demonstrated the powerful adsorption of TA on the hematite surface (chemical adsorption). At pH 9.2, since the hematite surface and TA have a high negative charge, electrostatic repulsion would have occurred between them. Still, the presence of dense Fe sites on the hematite surface and their high affinity to interact with TA, led to overcoming the repulsive forces. As a result, the TA strong interaction with the mineral surface of hematite would be expected.

## 3.6. FT-IR analysis

The FT-IR spectrum for TA is presented in Fig. 10-a. In the FT-IR spectrum of TA, the band at  $3404~\rm cm^{-1}$  is related to the phenolic –OH stretching vibration. Two peaks at  $2919~\rm cm^{-1}$  and  $2852~\rm cm^{-1}$  belong to the CH stretching vibrations. The bands at  $1617~\rm cm^{-1}$ ,  $1341~\rm cm^{-1}$ , and  $1456~\rm cm^{-1}$  are attributed to -C = C- of the aromatic ring, carboxyl carbonyl (carbonyl group), and carboxylates groups (Mahiuddin et al., 1992; Zhang et al., 2012; Erdem et al., 2013; Muhoza et al., 2019). The absorption peak at  $1030~\rm cm^{-1}$  and the absorption peaks in the ranges  $844~\rm cm^{-1}$  to  $466~\rm cm^{-1}$  are assigned to the vibration of C–O–C and the C-H bands, respectively. With attention to TA characterization and the presence of oxygen-containing functional groups like carboxyl, phenolic, and hydroxyl in its chemical structure, there is a strong possibility of interaction between surfaces of metallic minerals with TA.

The FT-IR spectra of TA, pure hematite, and the hematite treated

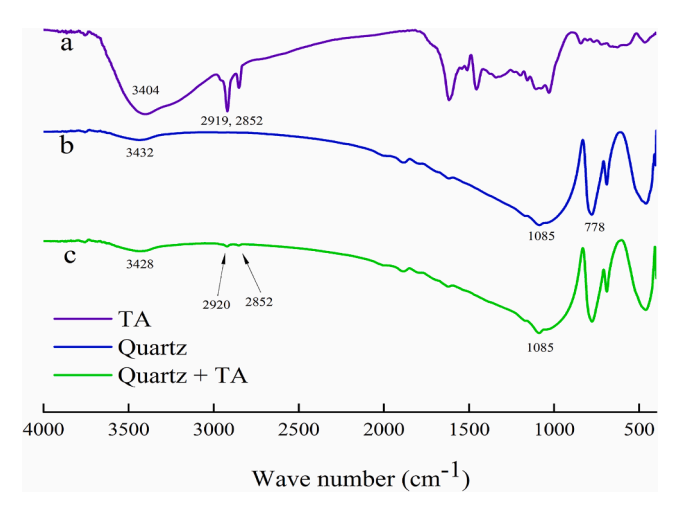


Fig. 11. FT-IR spectra of (a) TA, (b) quartz, and (c) quartz treated with 100 mg/L TA.

with TA (Fig. 10-b and c) showed the characteristic bands of hematite appeared at 469 cm<sup>-1</sup>, 553 cm<sup>-1</sup>, and 1025 cm<sup>-1</sup> corresponded to the Fe-O vibration (metal-O) and -OH stretching vibration (Pavlovic and Brandao, 2003). The newly emerged peak at 630 cm<sup>-1</sup> in the FT-IR spectrum of hematite after treatment with TA indicated the formation of a new band between Fe-O bonds located on the hematite surface and functional groups of TA containing hydrogen molecules (Fe-OH). The shifted and deformed peaks of 1025 cm<sup>-1</sup> to 896 cm<sup>-1</sup>, which were also strengthened after adsorption, potentially showed a strong chemical interaction between C-O stretch from carboxylic acids and the hematite surface. The band of 553 cm<sup>-1</sup> in the bare hematite spectrum shifted by 19 cm<sup>-1</sup> to 572 cm<sup>-1</sup>, represented the formation of a hydrogen band between the TA molecules and the hematite surface. Moreover, the O-H band of the blank hematite at 3423 cm<sup>-1</sup> shifted to 3413 cm<sup>-1</sup>. This indicates that phenol functional groups of TA are adsorbed on the hematite surface (H-bonding).

The TA treated hematite surface showed (Fig. 10) new peaks, which appeared at 2919 cm<sup>-1</sup> and 2851 cm<sup>-1</sup>, and attributed to the stretching vibrations of the  $-CH_2$  and  $-CH_3$  from the TA spectrum. These bonds confirmed that the TA molecules were adsorbed on the hematite surface. Four new peaks emerged at 1629 cm<sup>-1</sup>, 1564 cm<sup>-1</sup>, 1465 cm<sup>-1</sup>, and  $1394~{\rm cm}^{-1}$  could be carbonyl and carboxylate groups of TA that interacted with the hematite surface by chemisorption (Mahiuddin et al., 1992; Zhang et al., 2012, Tohry et al., 2021a). Since many TA peaks emerged in the hematite spectrum, it was deduced that TA was adsorbed on the surface of hematite by forming stable and powerful bands, something that was also confirmed in the adsorption experiments zeta potential measurements. Characteristic bands for quartz particles were observed at 1085 cm<sup>-1</sup>, 778 cm<sup>-1</sup>, and 458 cm<sup>-1</sup> (silanol groups and -OH corresponding bands) (Fig. 11). By treating quartz with TA, new characteristic peaks did not appear in the quartz + TA spectrum (Fig. 11c). However, new weak peaks of 2920 cm<sup>-1</sup> and 2852 cm<sup>-1</sup> were detected in the quartz + TA spectrum, which indicated the absorption of TA on the quartz surface. Moreover, a small shift (4 cm<sup>-1</sup>) without deformation can be observed in the surface of quartz after treating with TA (in the 3428 cm<sup>-1</sup>), which illustrated that TA interacted with the quartz surface by very weak H-bonding (physical interaction). These results were consistent with the adsorption and zeta potential results, where partial absorption of TA was observed on the quartz surface. Therefore, in the micro-flotation and surface wettability experiments, partial depressing of quartz particles and a minor decrease in their hydrophobicity were observed.

#### 4. Conclusion

The effect of TA and its adsorption mechanism on the hematite and quartz minerals in the reverse cationic flotation of iron oxides were investigated through micro-flotation, wettability, and various adsorption studies. Micro-flotation results of single pure minerals indicated that TA at a concentration of 100 mg/L and pH  $\sim$  9.2, in the presence of 30 mg/L ether amine, could selectively depress hematite and had a negligible effect on the quartz floatability. TA depressed more than 90% of hematite particles under these conditions and less than 8% of quartz particles. Mixture micro-flotation results also depicted that hematite could selectively separate from quartz, where only in one stage flotation, a concentrate with 66.6% Fe grade and 87.7% iron recovery could be achieved. Wettability analysis showed that the quartz hydrophobicity in the presence of Flotigam®EDA was higher than the hematite in the same condition. Floatability and work of adhesion of quartz in the presence of 30 mg/L Flotigam®EDA were 97.1% and 117.1 erg/cm<sup>2</sup> and for hematite 83.1% and 135.5 erg/cm<sup>2</sup>, respectively. The TA addition decreased hematite hydrophobicity (W<sub>a</sub> = 143.1 erg/cm<sup>2</sup>) much more than the quartz ( $W_a = 120.7 \text{ erg/cm}^2$ ).

Surface adsorption and zeta potential assessments demonstrated that a slight amount of TA was adsorbed on the quartz surface, compared to the TA amount that was adsorbed on the hematite surface. These outcomes were confirmed by Freundlich isotherm model constants, where n value for hematite and quartz was obtained 1.79 and 0.49, respectively (indicating stronger adsorption of TA on the hematite surface than the quartz). In agreement with adsorption and zeta potential outcomes, turbidity results illustrated that TA dispersed quartz particles in the suspension, while hematite particles were aggregated by adding the TA. This also resulted in the selective interaction of TA with hematite particles. FT-IR results illustrated that both H-bonding and strong chemisorption were the TA adsorption mechanisms on the hematite surface, while there was a poor physical TA adsorption on the quartz surface.

Regarding the TA promising depression effect on hematite particles through its reverse cationic flotation separation from quartz, exploring the effect of different condensed tannins on various hematites, based on their sources and liberation degree should be considered in the batch scale and by using high tech surface analyses such as Time-of-Flight Secondary Ion Mass Spectrometry (ToF-SIMS).

## CRediT authorship contribution statement

A. Tohry: Conceptualization, Methodology, Data curation, Writing original draft, Software, Validation, Writing - review & editing. R. Dehghan: Conceptualization, Writing - original draft, Visualization, Investigation, Funding acquisition, Supervision, Resources, Writing - review & editing. Laurindo de Salles Leal Filho: Conceptualization, Supervision, Project administration, Funding acquisition, Resources. S. Chehreh Chelgani: Data curation, Supervision, Writing - review & editing.

## **Declaration of Competing Interest**

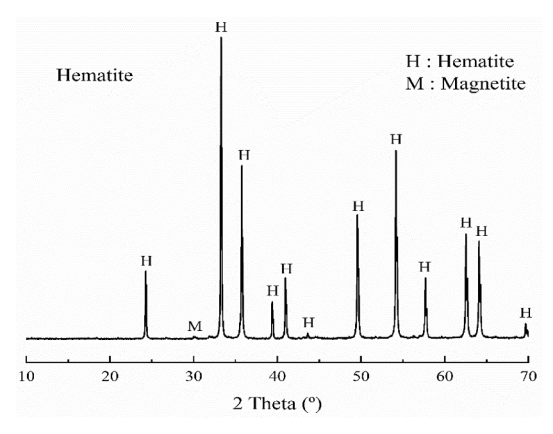
The authors declare that they have no known competing financial interests or personal relationships that could have appeared to influence the work reported in this paper.

## Acknowledgment

The first author would like to thank the Vale Institute of Technology (ITV) for providing financial support for the main parts of this work.

## Appendix A:. Characterization of material

See Fig. I See Tables I–III



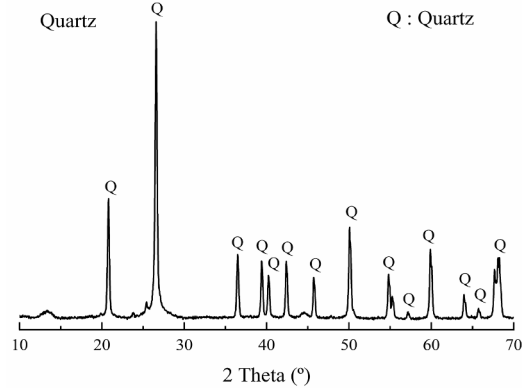


Fig. I. XRD patterns of the hematite and quartz.

**Table I**Chemical compositions of hematite and quartz samples (based on wt%).

Quartz 98.8 0.05 0.9 0.01 0.05 0.05 0.1 < 0.05 Hematite 0.34 68.7 < 0.2	Mineral	SiO <sub>2</sub> (%)	Al <sub>2</sub> O <sub>3</sub> (%)	Fe <sub>2</sub> O <sub>3</sub> (%)	MnO(%)	MgO(%)	CaO(%)	Na <sub>2</sub> O(%)	Others(%)	Fe(%)	FeO(%)
	Quartz Hematite	98.8 0.34								- 68.7	- < 0.2

**Table II**The distilled water analysis.

Salinity (EC 106)	T.D.S (ppm)	Co <sub>3</sub> <sup>2</sup> -(ppm)	Cl <sup>-</sup> (ppm)	So <sub>4</sub> <sup>2-</sup> (ppm)	Ca <sup>2+</sup> (ppm)	Mg <sup>2+</sup> (ppm)	Na <sup>+</sup> (ppm)	K <sup>+</sup> (ppm)	T.H (ppm)
< 2	< 1.2	N.D.	1.0	N.D.	0.3	0.2	0.8	0.2	2.5

**Table III**The deionized water analysis.

Elements	Ca <sup>2+</sup> (ppb)	Mg <sup>2+</sup> (ppb)	Fe <sup>3+</sup> (ppm)	Al <sup>3+</sup> (ppm)
De-ionized water	N.D.*	N.D.	N.D.	N.D.
Limit of detection	50.0	70.0	0.6	12.0

<sup>\*</sup> Not detecded.

#### References

- Abdel-Khalek, N.A., Yassin, K.E., Selim, K.A., Rao, K.H., Kandel, A.H., 2012. Effect of starch type on selectivity of cationic flotation of iron ore. Miner. Proces. Ext. Metal. 121 (2), 98–102. https://doi.org/10.1179/1743285512Y.0000000001.
- Al-Fariss, T.F., Ozbelge, H.O., El-Shall, H.S., 1992. On the phosphate rock beneficiation for the production of phosphoric acid in Saudi Arabia. J. King. Saud. Uni-Eng. Sci. 4 (1), 13–31. https://doi.org/10.1016/S1018-3639(18)30553-1.
- Araujo, A.C., Viana, P.R.M., Peres, A.E.C., 2005. Reagents in iron ores flotation. Miner. Eng. 18 (2), 219–224. https://doi.org/10.1016/j.mineng.2004.08.023.
- Audi, E.A., Toledo, D.P., Peres, P.G., Kimura, E., Pereira, W.K.V., de Mello, J.C.P., Nakamura, C., Alves-do-Prado, W., Cuman, R.K.N., Bersani, C.A., 1999. Gastric antiulcerogenic effects of Stryphnodendron adstringens in rats. Phytother. Res. 13, 264–266. https://doi.org/10.1002/(SICI)1099-1573(199905)13:3<264::AID-PTR443>3.0.C0:2-R.
- Bai, S., Ding, Z., Fu, X., Li, C., Lv, C., Wen, C., 2019. Investigations on soluble starch as the depressant of hematite during flotation separation of apatite. Phys. Prob. Miner. Process. 55 https://doi.org/10.5277/ppmp18108.
- Buah, W.K., Asamoah, R.K., Boadi, I., 2015. Effects of Quebracho Tannin on Recovery of Colloidal Gold from Bioleached Wash Liquor. Ghana Min. J. 15, 44–49.
- Carlson, J.J., Kawatra, S.K., 2013. Factors affecting zeta potential of iron oxides. Miner. Process. Ext. Metall. Rev. 34 (5), 269–303. https://doi.org/10.1080/08827588.2011.604607
- Churaev, N.V., Sergeeva, I.P., Sobolev, V.D., Jacobasch, H.-J., WeideNhammer, P., Schmitt, F.J., 2000. Modification of quartz surfaces using cationic surfactant solutions. Col. And Sur. A: Phys. And Eng. Asp. 164, 121–129. https://doi.org/10.1016/S0927-7757(99)00031-X.
- Chen, J., Li, Y., Long, Q., Wei, Z., Chen, Y., 2011. Improving the selective flotation of jamesonite using tannin extract. Int. J. Miner. Process. 100 (1–2), 54–56. https://doi. org/10.1016/j.minpro.2011.04.010.
- Conliffe, J., 2014. The Sawyer Lake iron-ore deposit, western Labrador: Potential for future high-grade iron-ore deposits in the Labrador Trough. Current Research. Government of Newfoundland and Labrador, Department of Natural Resources, Geological Survey, Report, 1-14.
- Davidson, M.S., 2009. An investigation of copper recovery from a sulphide oxide ore with a mixed collector system. Masters Abstr. Int. 49 (02). http://hdl.handle.net/ 1074/1074.
- Dos Santos, I.D., Oliveira, J.F., 2007. Utilization of humic acid as a depressant for hematite in the reverse flotation of iron ore. Miner. Eng. 20, 1003–1007. https://doi. org/10.1016/j.mineng.2007.03.007.
- Erdem, P., Bursali, E.A., Yurdakoc, M., 2013. Preparation and characterization of tannic acid resin: study of boron adsorption. Env. Prog. Sust. Energy. 32, 1036–1044. https://doi.org/10.1002/ep.11703.
- Engwayu, J., 2015. Aggregation and dispersion phenomena in the quartz-hematite system in the presence of polymers. Doctoral dissertation, University of British Columbia. https://dx.doi.org/10.14288/1.0165836.
- Fan, G., Wang, L., Cao, Y., Li, C., 2020. Collecting Agent-Mineral Interactions in the Reverse Flotation of Iron Ore: A Brief Review. Minerals 10 (8), 681. https://doi.org/
- Filippov, L.O., Filippova, I.V., Severov, V.V., 2010. The use of collectors mixture in the reverse cationic flotation of magnetite ore: The role of Fe-bearing silicates. Miner. Eng. 23 (2), 91–98. https://doi.org/10.1016/j.mineng.2009.10.007.
- Filippov, L.O., Severov, V.V., Filippova, I.V., 2013. Mechanism of starch adsorption on Fe-Mg-Al-bearing amphiboles. Int. J. Miner. Process. 123, 120–128. https://doi.org/ 10.1016/j.
- Filippov, L.O., Severov, V.V., Filippova, I.V., 2014. An overview of the beneficiation of iron ores via reverse cationic flotation. Int. J. Miner. Process. 127, 62–69. https://doi.org/10.1016/j.minpro.2014.01.002.
- Fraga-Corral, M., García-Oliveira, P., Pereira, A.G., Lourenço-Lopes, C., Jimenez-Lopez, C., Prieto, M.A., Simal-Gandara, J., 2020. Technological application of tannin-based extracts. Molecules 25 (3), 614. https://doi.org/10.3390/molecules25030614.
- Garcia, D.E., Glasser, W.G., Pizzi, A., Paczkowski, S.P., Laborie, M.P., 2016. Modification of condensed tannins: from polyphenol chemistry to materials engineering. New J. Chem. 40 (1), 36–49. https://doi.org/10.1039/C5NJ02131F.
- Gu, G., Chen, Z., Zhao, K., Song, S., Li, S., Wang, C., 2019. The effect of a novel depressant on the separation of talc and copper–nickel sulfide ore. Phys. Prob. Miner. Process. 55 https://doi.org/10.5277/ppmp18115.
- Gurung, M., Adhikari, B.B., Kawakita, H., Ohto, K., Inoue, K., Alam, S., 2012. Selective Recovery of Precious Metals from Acidic Leach Liquor of Circuit Boards of Spent Mobile Phones Using Chemically Modified Persimmon Tannin Gel. Ind. Eng. Chem. Res. 51, 11901–11913. https://doi.org/10.1021/ie3009023.
- Han, G., Wen, S., Wang, H., Feng, Q., 2020. Interaction mechanism of tannic acid with pyrite surfaces and its response to flotation separation of chalcopyrite from pyrite in

- a low-alkaline medium. J. Mater. Rese. Tech. 9 (3), 4421–4430. https://doi.org/10.1016/j.imrt.2020.02.067.
- Hem, J. D., 1960. Complexes of ferrous iron with tannic acid. US Government Printing Office. https://doi.org/10.3133/wsp1459D.
- Houot, R., 1983. Beneficiation of iron ore by flotation—review of industrial and potential applications. Int. J. Miner. Process. 10 (3), 183–204. https://doi.org/10.1016/0301-7516(83)00010.8
- Gibson, B., Wonyen, D.G., Chelgani, S.C., 2017. A review of pretreatment of diasporic bauxite ores by flotation separation. Miner. Eng. 114, 64–73. https://doi.org/ 10.1016/j.mineng.2017.09.009.
- Kar, B., Sahoo, H., Rath, S.S., Das, B., 2013. Investigations on different starches as depressants for iron ore flotation. Miner. Eng. 49 (2013), 1–6. https://doi.org/ 10.1016/j.mineng.2013.05.004.
- Konovalov, I.V., 1970. Origin of the Yeravninskiy iron ore deposits. Int. Geo. Rev. 12 (1), 87–95. https://doi.org/10.1080/00206817009475211.
- Krishna, S.J.G., Patil, M.R., Rudrappa, C., Kumar, S.P., Ravi, B.P., 2013. Characterisation and Processing of Some Iron Ores of India. J. Inst. Eng. (India): Ser. D 94 (2), 113–120. https://doi.org/10.1007/s40033-013-0030-4.
- Laskowski, J.S., 1989. The colloid chemistry and flotation properties of primary aliphatic amines. In: Sastry, K.V.S., Fuerstenau, M.C. (Eds.), Chall. In. Miner. Process. SME, Littleton, CO, pp. 15–34.
- Leja, J., Surface chemistry of froth flotation. 1st edition, Springer, 1982. 10.1007/978-1-4615-7975-5.
- Lelis, D.F., Leão, V.A., Lima, R.M.F., 2016. Effect of EDTA on quartz and hematite flotation with starch/amine in an aqueous solution containing Mn<sup>2+</sup> ions. REM-Int. Eng. J. 69 (4), 479–485. https://doi.org/10.1590/0370-44672016690014.
- Lelis, D.F., da Cruz, D.G., Fernandes Lima, R.M., 2019. Effects of calcium and chloride ions in iron ore reverse cationic flotation: Fundamental studies. Miner. Process. Extr. Metal. Rev. 40 (6), 402–409. https://doi.org/10.1080/08827508.2019.1666122.
- Lelis, D.F., Fernandes Lima, R.M., Rocha, G.M., Leão, V.A., 2020. Effect of Magnesium Species on Cationic Flotation of Quartz from Hematite. Miner. Process. Ext. Metal. Rev. 1–7 https://doi.org/10.1080/08827508.2020.1864362.
- Li, M., Yuan, Q., Gao, X., Hu, Y., 2020. Understanding the differential depression of tetrasodium glutamate diacetate on the separation of specularite and chlorite: Experimental and DFT study. Miner. Eng. 159, 106629 https://doi.org/10.1016/j. mineng.2020.106629.
- Liu, C., Feng, Q., Zhang, G., Chen, W., Chen, Y., 2016. Effect of depressants in the selective flotation of scheelite and calcite using oxidized paraffin soap as collector. Int. J. Miner. Process. 157, 210–215. https://doi.org/10.1016/j. minpro.2016.11.011.
- Liu, W., Wang, X., Xu, H., Miller, J.D., 2017. Physical chemistry considerations in the selective flotation of bastnaesite with lauryl phosphate. Miner. Metal. Process. 34 (3), 116–124. https://doi.org/10.19150/mmp.7611.
- Lu, Y., Liu, W., Wang, X., Cheng, H., Cheng, F., Miller, J.D., 2020. Lauryl Phosphate Flotation Chemistry in Barite Flotation. Minerals 10 (3), 280. https://doi.org/ 10.3390/min10030280.
- Ma, X., Marques, M., Gontijo, C., 2011. Comparative studies of reverse cationic/anionic flotation of Vale iron ore. Inter. J. Miner. Process. 100 (3–4), 179–183. https://doi. org/10.1016/j.minpro.2011.07.001.
- Ma, M., 2012. The significance of dosing sequence in the flocculation of hematite. Chem. Eng. Sci. 73, 51–54. https://doi.org/10.1016/j.ces.2012.01.031.
- Mahiuddin, S., Suryanarayan, I., Dutta, N.N., Borthakur, P.C., 1992. Adsorption studies of sodium humate on Indian iron ore fines. Col. Surf. 64 (3–4), 177–184. https://doi. org/10.1016/0166-6622(92)80097-1.
- C. Malan, C., 2015. Review: humic and fulvic acids. A Practical Approach, Sust. Soil. Manag. Symp. Stellenbosch. 5-6.
- Manser, R.M., 1975. Handbook of silicate flotation. Warren Spring Laboratory, Stevenage, Herts.
- Martinz, M., 2009. Apatite wettability and its influence on flotation, Ph.D thesis, University of Sao Paulo (in Portuguese).
- Matveeva, T.N., Gromova, N.K., Lantsova, L.B., 2016. Adsorption of tannin-bearing organic reagents on stibnite, arsenopyrite and chalcopyrite in complex gold ore flotation. J. Min. Sci. 52 (3), 551–558. https://doi.org/10.1016/j. colsurfa.2008.10.004.
- Matveeva, T.N., Gromova, N.K., Lantsova, L.B., 2017. Effect of Tannin on compound collector adsorption and stibnite and arsenopyrite flotation from complex ore.
  J. Min. Sci. 53 (6), 1108–1115. https://doi.org/10.1134/S1062739117063197.
- Meng, Q., Yuan, Z., Xu, Y., Du, Y., 2019. The effect of sodium silicate depressant on the flotation separation of fine wolframite from quartz. Sep. Sci. Tech. 54 (8), 1400–1410. https://doi.org/10.1080/01496395.2018.1533870.
- Ming, P., Xie, Z., Guan, Y., Wang, Z., Li, F., Xing, Q., 2020. The effect of polysaccharide depressant xanthan gum on the flotation of arsenopyrite from chlorite. Miner. Eng. 157, 106551 https://doi.org/10.1016/j.mineng.2020.106551.
- Mphela, N., 2010. Fundamental studies of the electrochemical and flotation behaviour of pyrrhotite. Doctoral dissertation, University of Pretoria. http://hdl.handle.net/22
- Muhoza, B., Xia, S.Q., Zhang, X.M., 2019. Gelatin and high methyl pectin coacervates crosslinked with tannic acid: the characterization, rheological properties, and application for peppermint oil microencapsulation. Food. Hydrocoll. 97, 105174 https://doi.org/10.1016/j.foodhyd.2019.105174.
- Norgren, M., Lindström, B., 2000. Dissociation of phenolic groups in kraft lignin at elevated temperatures. Wood. Res. Tech. 54 (5), 519–527. https://doi.org/10.1515/
- Noro, T., Ohki, T., Noda, Y., Warashina, T., Noro, K., Tomita, I., Nakamura, Y., 1999. Inhibitory effect of hydrolysable tannins on tumor promoting activities of 12-O-tetradecanoylphorbol-13-acetate (TPA) in JB6 mouse epidermal cells. Kluwer

- Academic/Plenum Publishers, New York, NY, USA, pp. 665–674. https://doi.org/10.1007/978-1-4615-4139-4-37.
- Nunes, A.P.L., Peres, A.E.C., De Araujo, A.C., Valadão, G.E.S., 2011. Electrokinetic properties of wavellite and its floatability with cationic and anionic collectors. J. Col. Interf. Sci. 361 (2), 632–638. https://doi.org/10.1016/j.jcis.2011.06.014.
- Pavlovic, S., Brandao, P.R.G., 2003. Adsorption of starch, amylose, amylopectin and glucose monomer and their effect on the flotation of hematite and quartz. Miner. Eng. Froth Flotation. 16, 1117–1122. https://doi.org/10.1016/j. minerg.2003.06.011.
- Pearse, M.J., 2005. An overview of the use of chemical reagents in mineral processing. Miner. Eng. 18 (2), 139–149. https://doi.org/10.1016/j.mineng.2004.09.015.
- Peçanha, E.R., Albuquerque, M.D.D.F., Simão, R.A., De Salles Leal Filho, L., Mello Monte, M.B., 2019. Interaction forces between colloidal starch and quartz and hematite particles in mineral flotation. Col. Surf. A: Phys. Eng. Asp. 562, 79–85. https://doi.org/10.1016/j.colsurfa.2018.11.026.
- Pinto, C.L.L., De Araujo, A.C., Peres, A.E.C., 1992. The effect of starch, amylose and amylopectin on the depression of oxi-minerals. Miner. Eng. 5 (3–5), 469–478. https://doi.org/10.1016/0892-6875(92)90226-Y.
- Pizzi, A., 1983. Tannin-based wood adhesives. In. Wood. Adh. Chem. Tech. 1, 178–246. https://doi.org/10.1007/978-1-4684-7511-1\_29.
- Pizzi, A., 2008. Tannins: Major Sources, Properties and Applications. Elsevier, Oxford, UK, pp. 179–199.
- Pizzi, A., 2019. Tannins: Prospectives and actual industrial applications. Biomolecules 9 (8), 344. https://doi.org/10.3390/biom9080344.
- Poperechnikova, O.Y., Filippov, L.O., Shumskaya, E.N., Filippova, I.V., 2017. Intensification of the reverse cationic flotation of hematite ores with optimization of process and hydrodynamic parameters of flotation cell. Int. J. Physic: Conf. Ser. 879 (1), 012016.
- Raju, G.B., Holmgren, A., Forsling, W., 1998. Complexation mechanism of dextrin with metal hydroxides. J. Col. Interf. Sci. 200 (1), 1–6. https://doi.org/10.1006/ icis.1997.5332.
- Ramakgala, C., Danha, G., 2019. Mineralogical characterisation of Matsitama banded iron ore. IOP Conf. Ser.: Mater. Sci. Eng. 641 (1), 012029 https://doi.org/10.1088/ 1757-899X/641/1/012029.
- Ramos-Tejada, M.M., Ontiveros, A., Viota, J.L., Durán, J.D.G., 2003. Interfacial and rheological properties of humic acid/hematite suspensions. J. Col. Interf. Sci. 268, 85–95. https://doi.org/10.1016/S0021-9797(03)00665-9.
- Rodrigues, W.J., Leal Filho, L.S., 2010. Importance of hydrodynamics in coarse particle flotation kinetics. Rem-Revista Escola De Minas. 63 (4), 615–620. https://doi.org/ 10.1590/S0370-44672010000400003.
- Rutledge, J., Anderson, C.G., 2015. Tannins in mineral processing and extractive metallurgy. Metals 5 (3), 1520–1542. https://doi.org/10.3390/met5031520.
- Rutledge, J., 2016. Fundamental surface chemistry and froth flotation behavior using quebracho tannins. Master's Thesis, Colorado School of Mines, Golden, CO, USA.
- Sarquís, P.E., Menéndez-Aguado, J.M., Mahamud, M.M., Dzioba, R., 2014. Tannins: the organic depressants alternative in selective flotation of sulfides. J. Clean. Prod. 84, 723–726. https://doi.org/10.1016/j.jclepro.2014.08.025.
- Severov, V.V., Filippov, L.O., Filippova, I.V., 2016. Relationship between cation distribution with electrochemical and flotation properties of calcic amphiboles. Int. J. Miner. Process. 147, 18–27. https://doi.org/10.1016/j.minpro.2015.12.005.
- Schulz, N.F., Cooke, S.R., 1953. Froth Flotation of Iron Ores. Adsorption of Starch Products and Laurylamine Acetate. Ind. Eng. Chem. 45 (12), 2767–2772. https://doi.org/10.1021/je50528a057.
- Seifelnassr, A.A., Moslim, E.M., Abouzeid, A.Z.M., 2013. Concentration of a Sudanese low-grade iron ore. Int. J. Miner. Process. 122, 59–62. https://doi.org/10.1016/j. minro 2013 04 001
- Shrimali, K., Miller, J.D., 2016. Polysaccharide depressants for the reverse flotation of iron ore. Trans. Indi. Inst. Met. 69 (1), 83–95. https://doi.org/10.1007/s12666-015-0708-4.
- Shrimali, K., Atluri, V., Wang, Y., Bacchuwar, S., Wang, X., Miller, J.D., 2018. The nature of hematite depression with corn starch in the reverse flotation of iron ore. J. Col. Interf. Sci. 524, 337–349. https://doi.org/10.1016/j.jcis.2018.04.002.
- Siame, M.C., Kaoma, J., Shibayama, A., 2019. Development of impurities removal process for low grade Sanje iron ore using mineral processing technologies. J. Nat. App. Sci. 3 (1), 36–52.
- Silva, E.M.S., Peres, A.E.C., Silva, A.C., Florencio, D.L., Caixeta, V.H., 2019. Sorghum starch as depressant in mineral flotation: part 2-flotation tests. J. Mater. Res. Tech. 8 (1), 403–410. https://doi.org/10.1016/j.jmrt.2018.04.002.
- Smith, R.W., 1963. Coadsorption of dodecylamine ion and molecule on quartz. Trans. SME/AIME 226, 427–433.

- Smith, R.W., Scott, J.L., 1990. Mechanisms of dodecylamine flotation of quartz. Miner. Process. Ext. Metal. Rev. 7 (2), 81–94. https://doi.org/10.1080/ 08827509008952667.
- Smith, M.B., March, J., 2007. Advanced Organic Chemistry: Reactions, Mechanisms, and Structure, sixth ed. Wiley-Interscience, New York.
- Song, S., Lu, S., Lopez-Valdivieso, A., 2002. Magnetic separation of hematite and limonite fines as hydrophobic flocs from iron ores. Miner. Eng. 15 (6), 415–422. https://doi.org/10.1016/S0892-6875(02)00054-7.
- Souza, T.F., Lima, R.M.F., 2019. Cationic flotation of smithsonite and dolomite from Brazilian Ambrósia Norte Deposit. REM-Int. Eng. J. 72 (4), 619–624. https://doi. org/10.1590/0370-44672019720009.
- Tangarfa, M., Semlali Aouragh Hassani, N., Alaoui, A., 2019. Behavior and mechanism of tannic acid adsorption on the calcite surface: isothermal, kinetic, and thermodynamic studies. ACS Omega 4 (22), 19647–19654. https://doi.org/ 10.1021/acsomega.9b02259.
- Tohry, A., Dehghani, A., 2016. Effect of sodium silicate on the reverse anionic flotation of a siliceous–phosphorus iron ore. Sep. Pur. Tech. 164, 28–33. https://doi.org/10.1016/j.seppur.2016.03.012.
- Tohry, A., Dehghan, R., Chehreh Chelgani, S., Rosenkranz, J., Rahmani, O.A., 2019. Selective Separation of Hematite by a Synthesized Depressant in Various Scales of Anionic Reverse Flotation. Minerals 9 (2), 124. https://doi.org/10.3390/ min9020124.
- A. Tohry R. Dehghan A.V. Oliveira S.C. Chelgani L. de Salles Leal Filho Enhanced Washburn Method (EWM): A comparative study for the contact angle measurement of powders Adv. Pow. Tech. 31 12 2020 4665 4671 10.1016/j.apt.2020.10.014.
- Tohry, A., Dehghan, A., Zarei, M., Chelgani, S.C., 2021a. Mechanism of humic acid adsorption as a flotation separation depressant on the complex silicates and hematite. Miner. Eng. 162, 106736 https://doi.org/10.1016/j.mineng.2020.106736.
- Tohry, A., Dehghan, R., Hatefi, P., Chelgani, S.C., 2021b. A comparative study between the adsorption mechanisms of sodium co-silicate and conventional depressants for the reverse anionic hematite flotation. Sep. Sci. Tech. 1–18. https://doi.org/ 10.1080/01496395.2021.1887893.
- Turrer, H.D.G., Peres, A.E.C., 2011. Investigation on alternative depressants for iron ore flotation. Miner. Eng. 23 (2011), 1066–1069. https://doi.org/10.1016/j. minerg.2010.05.009.
- Veloso, C.H., Filippov, L.O., Filippova, I.V., Ouvrard, S., Araujo, A.C., 2018. Investigation of the interaction mechanism of depressants in the reverse cationic flotation of complex iron ores. Miner. Eng. 125, 133–139. https://doi.org/10.1016/j. mineng.2018.05.031.
- Vidyadhar, A., Rao, K.H., Chernyshova, I.V., Forssberg, K.S.E., 2002. Mechanisms of amine-quartz interaction in the absence and presence of alcohols studied by spectroscopic methods. J. Col. Interf. Sci. 256 (1), 59–72. https://doi.org/10.1006/ icis.2001.7895.
- Vieira, A.M., Peres, A.E., 2007. The effect of amine type, pH, and size range in the flotation of quartz. Miner. Eng. 20 (10), 1008–1013. https://doi.org/10.1016/j. mineng.2007.03.013.
- Yu, B., Zhang, Y., Shukla, A., Shukla, S.S., Dorris, K.L., 2001. The removal of heavy metals from aqueous solutions by sawdust adsorption - removal of lead and comparison of its adsorption with copper. J. Hazard. Mat. 84, 83–94. https://doi. org/10.1016/S0304-3884(01)00198-4
- Zhang, L., Wang, Z.L., Li, Z.Q., Zhang, L., Xu, Z.C., Zhao, S., Yu, J.Y., 2010. Wettability of a quartz surface in the presence of four cationic surfactants. Langmuir 26 (24), 18834–18840. https://doi.org/10.1021/la1036822.
- Zhang, Y.B., Li, P., Zhou, Y.L., Han, G.H., Li, G.H., Xu, B., Jiang, T., 2012. Adsorption of lignite humic acid onto magnetite particle surface. J. Cent. S. Uni. 19 (7), 1967–1972. https://doi.org/10.1007/s11771-012-1233-9.
- Zhang, X., Gu, X., Han, Y., Parra-Álvarez, N., Claremboux, V., Kawatra, S.K., 2019. Flotation of iron ores: A review. Miner. Process. Ext. Metal. Rev. 1–29. https://doi.org/10.1080/08827508.2019.1689494.
- Zhao, K., Yan, W., Wang, X., Hui, B., Gu, G., Wang, H., 2017. The flotation separation of pyrite from pyrophyllite using oxidized guar gum as depressant. Int. J. Miner. Process. 161, 78–82. https://doi.org/10.1016/j.minpro.2017.02.015.
- Zhou, Y., Zhang, Y., Li, P., Li, G., Jiang, T., 2014. Comparative study on the adsorption interactions of humic acid onto natural magnetite, hematite and quartz: effect of initial HA concentration. Pow. Tech. 251, 1–8. https://doi.org/10.1016/j. powtec.2013.10.011.
- Zhou, Y., Zhang, Y., Li, G., Wu, Y., Jiang, T., 2015. A further study on adsorption interaction of humic acid on natural magnetite, hematite and quartz in iron ore pelletizing process: Effect of the solution pH value. Pow. Tech. 271, 155–166. https://doi.org/10.1016/j.powtec.2014.10.045.